Available online at www.sciencedirect.com

ScienceDirect

Nuclear and Particle Physics Proceedings 273–275 (2016) 1147–1154

www.elsevier.com/locate/nppp

# Upgrade of the CMS Instrumentation for luminosity and machine induced background measurements

Anne Dabrowski for the CMS Collaboration

*CERN, CH-1211 Geneva 23, Switzerland*

**Abstract**

To optimise performance with the higher luminosity, higher beam energy and shorter bunch spacing of 25 ns at the LHC after 2014, an upgrade program is performed for the detectors to measure the luminosity and machine induced background. A new detector is the pixel luminosity telescope consisting of 8 telescopes, equipped with silicon pixel sensors, on both ends of the interactions point. The Fast Beam Conditions Monitoring system, using diamond sensors, is upgraded to 24 sensors, 12 on each end of the IP. In addition, dedicated fast ASICs produced in 130 nm commercial CMOS technology and dead-time free backend electronics using FPGAs for fast signal processing are being developed and built. Also, the part of the forward HCAL used for the luminosity measurement is instrumented with new readout electronics, in microTCA standards. The machine induced background measurement will be supported by a new system of direction sensitive quartz Cherenkov counters, with excellent time resolution. A data acquisition architecture is being developed that is common for all subsystems and allows for synchronization across different hardware. The design of the new system will be presented, and a report will be given on the performance of each subsystem measured in several test-beam campaigns and prototype operation in the last LHC run.

*Keywords:*
luminosity, beam, monitoring, LHC, CMS, background

## 1. Introduction

The Compact Muon Solenoid (CMS) detector [1] is one of two general purpose detectors at the Large Hadron Collider (LHC) [2] at CERN. During LHC Run I (2010-2012 running period), proton-proton beam collided at a centre-of-mass energy up to 8 TeV with 50 ns bunch spacing. The instantaneous luminosity reached more than $7 \times 10^{33}\text{cm}^{-2}\text{s}^{-1}$ and about 30 $fb^{-1}$ of integrated luminosity was delivered to CMS.

To ensure safe, high quality data-taking conditions for the CMS detector and to optimize and account for the luminosity delivered for physics during Run II, upgraded instrumentation is designed to monitor the LHC beam conditions for CMS. These systems are being installed during the 2013-2014 period of LHC scheduled maintenance, Long Shutdown 1 (LS1). The systems have been optimized to measure the per-bunch online luminosity and the machine-induced background (MIB) for the CMS experiment, for the beam conditions expected in Run II. The LHC will re-start operations in Run II with proton-proton collisions at a centre-of-mass energy of 13 TeV and bunch spacing of 25 ns. A peak luminosity of $1.4 \times 10^{34}$ cm$^{-2}$ s$^{-1}$ will be achieved during the first year and then reach $2 \times 10^{34}\text{cm}^{-2}\text{s}^{-1}$ with around 50 interactions per bunch crossing, twice the instantaneous luminosity foreseen in the initial LHC technical design report.

The luminosity is a key parameter of a collider experiment as higher values allow an exploration of lower cross section processes. Its precise measurement is necessary to determine cross sections. In addition, from the integrated luminosity the dose load to the detector components is inferred. The online luminometers include

http://dx.doi.org/10.1016/j.nuclphysbps.2015.09.180
2405-6014/

the Pixel Luminosity Telescope (PLT) described in Section 2, the Fast Beam Conditions Monitor (BCM1F), described in Section 3, and the luminosity based on a dedicated readout of the Hadron Forward (HF) Calorimeter described in Section 4. These online luminometers are independent and together with the highly linear offline luminosity measurement based on pixel cluster counting, allow for a cross check and reduction of the systematic errors.

The higher beam intensity implies tighter collimator settings and an increased susceptibility to electron cloud effects contributing to a higher potential for MIB for CMS. The upgraded Fast Beam Conditions Monitor (BCM1F), as described in Section 3, is designed to have sensitivity at low radius where beam gas interactions near CMS will be detected. The Beam Halo Monitor (BHM), as described in Section 5, will have sensitivity towards distant distant beam gas and beam halo interactions with the collimators.

To fully exploit the redundant online luminosity and beam background measurement system, the BRIL subsystems are synchronized using common timing signals distributed by the CMS Trigger, Control and Distribution System (TCDS). A common architecture for the data acquisition is being developed based on the CMS XDAQ online software framework to ease data exchange, storage, monitoring, database management and the maintainability of the readout software across systems and will be described in detail in Section 6.

This paper will present the design of the upgrades of the beam monitoring systems by the CMS BRIL project during LS1, as summarised in Figure 1.

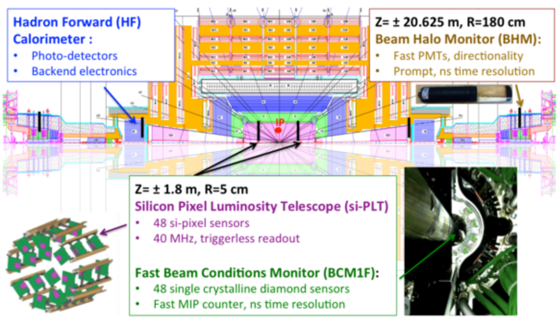


Figure 1: An overview of the upgraded CMS beam instrumentation sub-systems and their location in the CMS detector

## 2. Pixel Luminosity Telescope

The Silicon Pixel Luminosity Telescope (PLT) is a dedicated luminometer monitor for CMS based on silicon pixel sensors [3], as used in the CMS barrel pixel detector, bump bonded to the PSI46v2 CMS pixel readout chip [4] (ROC). The functionality and readout of this detector is based on an earlier design [5] that used uncooled single crystalline CVD pixelated diamond sensors.

The PLT is comprised of two arrays of eight small-angle telescopes situated one on each end of CMS, 1.75 m from the CMS interaction point (IP). Each telescope consists of three equally spaced planes of pixel sensors with a total telescope length of 7.5 cm and are located 5 cm radially from the beam line. The PLT is designed to provide a measurement of the bunch-by-bunch luminosity at the CMS collision point on a time scale of a few seconds and a high-precision measurement of the integrated luminosity.

The primary luminosity measurement of the PLT is based on counting the number of telescopes with threefold coincidences formed from the fast-or of the column-multiplicity signal output by the PSI46v2 readout chip. The fast-or signal, clocked at the bunch crossing frequency of 40 MHz, indicates the number of double columns with pixels over threshold in each bunch crossing. In addition, the full hit information consisting of the row and column addresses and the pulse heights of all signals over threshold is readout at a lower configurable frequency of a few kHz. This full pixel readout provides tracking information and is a powerful tool for determining systematic corrections, calibrating pixel efficiencies and measuring the collision point centroid as a function of time.

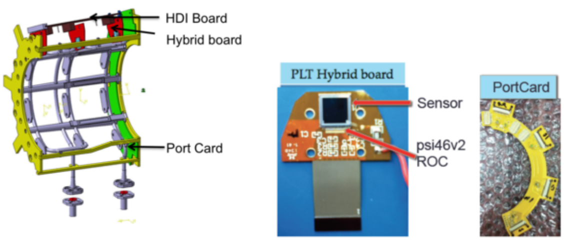


(a) (b)

Figure 2: (a) PLT cassette providing the frame for electronics, alignment components and cooling distribution (b) An example of the silicon PLT hybrid board and port card.

The PLT frontend hybrid boards, hosting the sensor and readout chip, are mounted onto the cassette as shown in Figure 2 (a), on the IP end of the carriage, as shown in Figure 3. The mechanics for the PLT detector and the hybrid boards were designed and produced during LS1 to incorporate the new requirement for provid-

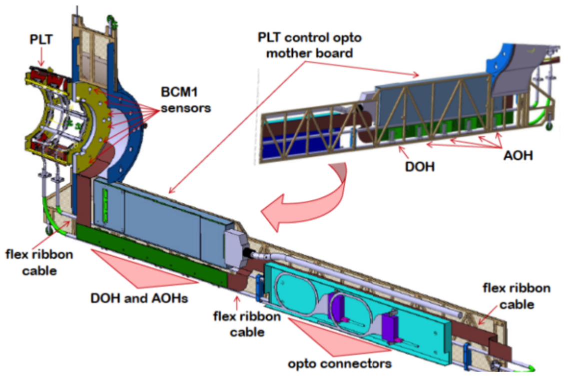


Figure 3: Drawings of the PLT and BCM1 support carriage, 1/4 of the detector system is shown, installed at a Z location of ±1.8 m from the IP, inside the pixel support tube.

ing a cooling distribution and performant thermal contact to the silicon sensors, as shown in Figure 3. The cassette was produced from a titanium alloy using the selective laser melting (SLM) technique. This structure has a hallow inner diameter of 2.8 mm allowing for the flow of C6F14 coolant qualified to a pressure of 15 bar.

Three hybrid board planes form a telescope and are connected by pigtails to the High Density Interconnect (HDI), a four-layer flex circuit. The HDI houses a CMS pixel Token Bit Manager (TBM) chip that communicates with the three readout chips in the telescope and orchestrates the readout of the full sensor information. A custom PLT driver chip amplifies and outputs the three fast-or signals onto separate analog lines. The HDI also distributes low voltage power and sensor bias voltage to the hybrid boards. The HDI circuits connect to a semi-circular port card board located at the end of the support carriage with one port card for each half carriage (four telescopes), as shown in Figure 2 (b).

The port card connects to the opto board a custom circuit, located at the foot of the carriage, shown in Figure 4 (a). The opto board houses the optical hybrid circuits for the outgoing analog signals (full signal readout of the pixels and fast-ors) and for the digital control signals. From the opto board the analog signal fibers connect to a Front End Driver (FED) [6], a VME flash ADC module, located in the CMS underground service cavern. The histogramming of the 40 MHz, fast-or signals is done in the PLT FED.

As for all BRIL subsystems, the firmware in the FED has been adapted to histogram the fast-or data based on a common time interval[1], so called "lumi-nibble", distributed by the CMS TCDS system.

A photo of the assembled cassette mounted onto the carriage is shown in Figure 4 (b).

[1]Typical interval of $2^{12}$ LHC orbits defines the integration period

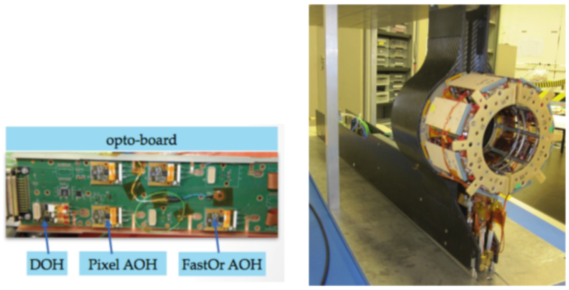


(a) (b)

Figure 4: (a) Optoboard for control and readout of full cassette (b) Two completed PLT cassette assemblies mounted to the carbon fibre support carriage.

## 3. Upgraded Fast Beams Conditions Monitor

### *3.1. Run I Configuration*

The Fast Beams Conditions Monitor (BCM1F) [7] has been in operation in CMS since 2008, successfully providing measurements of beam background [8] and a backup measurement of the online luminosity [10] for CMS. This BCM1F detector used in Run 1 consisted of 8 single crystalline CVD diamond sensors, with an active area of $5.0 \times 5.0\,\mathrm{mm}^2$, a thickness of $500\,\mu$m, located at a distance of 1.8 m from the interaction point at a radial distance of 5 cm. The sensors were coupled to a charge-sensitive, radiation-hard amplifier and shaper ASIC of the type JK16 [11] with a peaking time of 25 ns.

### *3.2. Upgraded BCM1F for Run II*

The upgrade of the BCM1F detector is driven by the requirement for efficient identification of collision and MIB signals at high rates and the requirement for sufficient radiation hardness. An average instantaneous charged particle flux of about $6 \times 10^7 \mathrm{cm}^{-2}\mathrm{s}^{-1}$ is predicted by FLUKA [12] calculations at the BCM1F detector location, for an instantaneous luminosity of $2 \times 10^{34} \mathrm{cm}^{-2}\mathrm{s}^{-1}$. The corresponding integrated hadronic fluence to the detector is predicted to exceed $6 \times 10^{14} \mathrm{cm}^{-2}$ hadrons, for $300\,\mathrm{fb}^{-1}$ of delivered luminosity. The upgrade of the detector comprises of two–pad sensors, dedicated frontend ASICs and the design of dead-time free backend electronics, with flexible FPGA for signal processing and sub-bunch histogramming capabilities.

### *3.2.1. BCM1 Frontend Upgrade*

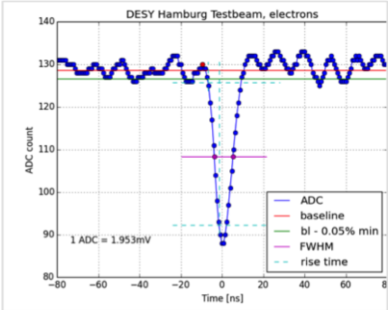


Figure 5: A MIP response from a test board containing the new fronted ASIC and a diamond sensor, measured in a test beam. The signal is digitised by an 8-bit ADCs with a 1.25 GS/s sampling rate.

To improve the time resolution of the detector, a new dedicated front-end ASIC has been developed at CERN in collaboration with the University of Science and Technology AGH Krakow. The ASIC is based on commercial IBM CMOS-8RF 130 nm technology and includes a fast trans-impedance preamplifier with an active feedback, a shaper stage and a fully differential output buffer. An charge-to-voltage conversion of 50 mV/fC is obtained which will improve the efficiency of particle detection. A FWHM of less than 10 ns is achieved for a MIP signal of 3 fC and less than 1k electrons ENC is measured. Each chip has 4 channels and a sophisticated calibration circuit to monitor the gain for 2 input levels corresponding to 1/2 and 1 MIP. The active feedback circuit allows for a fast recovery time (<30 ns), even for pulses with a large charge of up to 150 fC. The frontend was qualified in a test beam in DESY Hamburg with an electron beam, and a typical example of a MIP signal is shown in Figure 5.

The upgraded BCM1F detector acceptance is increased by a factor of three from an active area of *8* $5.0 \times 5.0\,mm^2$ sensors to *24* $5.0 \times 5.0\,mm^2$ sensors, to allow for additional statistical sensitivity to monitor the MIB. Each sensor, is metalised into two pads of approximately $5.0 \times 2.5\,mm^2$ (48 channels in total) to decrease the count rate per channel, and maintain linearity with increased pileup. The width of the gap between the two pads is $25\,\mu m$.

To house and bring services to 12 channels per 1/4 of the detector, a novel single integrated PCB has been produced made from flex and rigid parts, as shown in Figure 6 (a). Four such boards are required for the full detector assembly. This integrated PCB will host all passive and active components. The PCB has a complex, multilayer layout in order to fit all lines on the PCB and a limited volume inside the pixel service tube.

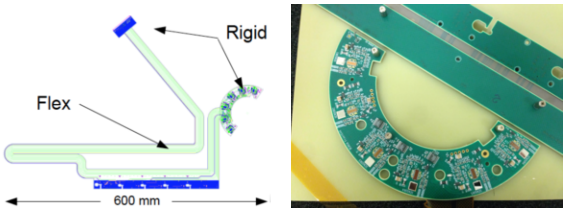


(a) BCM1 flat PCB (b) BCM1 half ring

Figure 6: Single integrated PCB for the BCM1F frontend upgrade.

This allows to have a connector free system, minimising the material budget in the pixel volume. The BCM1 PCB extended and mounted onto the support carriage is shown in Figure 3.

Onto the rigid half ring part of the PCB, are mounted six sCVD diamond sensors, metalized into two independent readout pads as shown in Figure 6 (b). The two readout pads are coupled to two input channels of the BCM1F ASIC. The central rigid PCB continues to a rectangular rigid PCB on the detector arm, through a flexible PCB. Onto this rectangular part is mounted the four, 3 channel analogue optohybrids [9] for optical signal transmission and a digital optohybrid for the slow control and settings of the gain and bias of the linear laser drivers. The mounting of the analogue optohybrids on to the detector arm, which is further away from the beam line than in Run I, lowering their exposure to radiation. The HV lines to the BCM1F sensors have been qualified to 1 kV. Operating the sensors at this voltage leads to less sensitivity to future radiation damage of the sCVD sensors.

### *3.2.2. BCM1 Backend Electronics Upgrade*

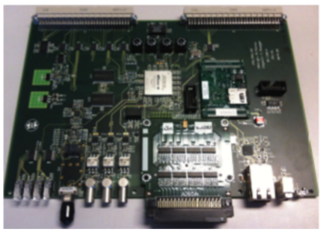

Figure 7: BCM1F VME Real-time histogram unit

The purpose of the backend electronics is to measure the arrival time and amplitude of all signals and associate the signals to either collision products or MIB for online per bunch luminosity and beam background measurements.

The BCM1F backend electronics strategy will retain the parallel path design from the Run I setup. Signals will be transmitted through the approximately 80 m of optical single mode fibers to the counting room where they are received by four 12-channel Analogue Receiver Modules (ARx12). The VME discriminator path will be used for initial running, while a MicroTCA digitizer system with fast peak-finding will be commissioned for future use.

The analog signal are fed to a VME discriminator with a double pulse resolution of 7 ns to measure the arrival time hit occupancy. The resulting digital signal are sent to a dedicated board, the Real-time histogramming unit (RHU) [13] and shown in Figure 7. The histograms are binned at four times the external bunch clock frequency, approximately 6.25 ns per bins, for 14,256 bins per orbit. The histogram integration interval is decoded from an optical timing signal received from the CMS TCDS system. The RHU provides double buffering and dead-time free processing of signals which is an important feature of an online luminosity system.

A copy of the discriminated signals are also sent to a multipurpose logic board to register hit coincidences between channels and to derive technical triggers for optimal tagging of underlying beam background events.

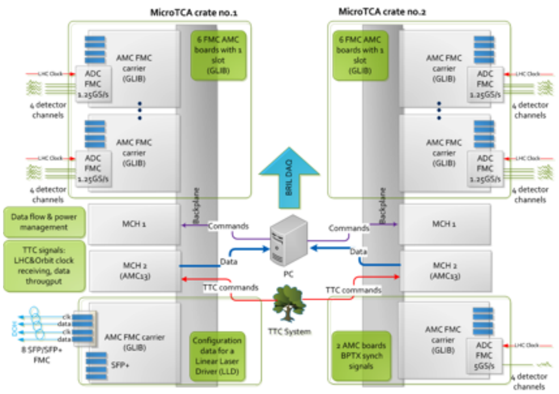


Figure 8: BCM1F MicroTCA electronics architecture and data flow.

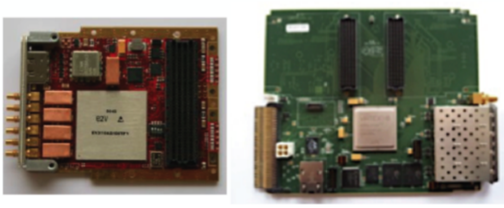

Figure 9: BCM1F MicroTCA electronics consisting of an 8-bit ADCs mezzanine ADC with 1.25GS/s sampling rate (left) and GLIB carrier board (right).

Complementing the VME electronics, a MicroTCA backend electronics architecture [14] is deployed to monitor the performance of the system and to exploit sophisticated online fast peak-finding algorithms to resolve overlapping signals at high pileup.

The trigger-less data flow and the system architecture is shown in Figure 8. The system control and communication will be operated by the specialized CMS MicroTCA Hub module AMC13 XG [15]. The module uses 10 Gb/s Ethernet based IPbus communication, suitable for transferring the large amount of the data. The analogue to digital conversion is performed by twelve 4-channel FMC mezzanines with 8-bit ADCs at a 1.25GS/s sampling rate (FMC125, 4DSP), mounted on the AMC carriers with single high-pin connector FMC connectors (GLIB), as shown in Figure 9. The external LHC clock will be provided to the mezzanines through the front panel to ensure ADC sample synchronisation. The 8-bit samples will be transmitted through FMC connectors to FPGAs mounted on the AMC carriers, that will host the firmware for the peak finding algorithms. The timing signals from the CMS TCDS will be decoded by the AMC13 modules and transmitted through the backplanes to all GLIB modules. The processing FPGA will use this information for creating the time stamps for the collected data. Amplitude and occupancy histograms will be collected during a Lumi Nibble. One orbit of a raw data per Lumi Nibble will be stored to provide an input for the offline statistic processing. During the storage time, without introducing any dead time, the data from a previous Lumi Nibble will be transmitted to the AMC13 through the backplane and subsequently to the BRIL DAQ.

## 4. Hadron Forward Calorimeter Upgrade for Luminosity Measurement

During Run I the HF tower occupancy method was the primary method used to perform high statistics, real-time bunch-by-bunch luminosity measurements for CMS. It is based on zero counting, in which the average fraction of empty towers is used to infer the mean number of interactions per bunch crossing. A second method, called "$E_T$ sum", exploits the linear relationship between the average transverse energy per tower and the luminosity. This algorithm has not yet been used, but is under consideration for Run II.

Two main activities in LS1, in the context of the HCAL Phase I upgrade program [16], affect the HF luminosity calibration and electronics: The first is the exchange of the photomultipliers and the second is an upgrade of the HF backend electronics. The upgrade of the

HF backend electronics in particular implies redevelopment of the HF luminosity firmware and DAQ during LS1.

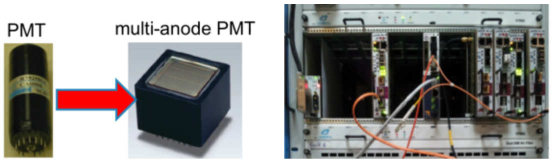


(a) HF PMT Upgrade (b) HF backend electronics crate

Figure 10: Upgrade of the HF frontend photodetectors (Hamamatsu R7600U-200-M4) and backend electronics using MicroTCA standard.

### *4.1. PMT Performance in Run I and Upgrade in LS1*

Time-dependent variations in the energy response of the HF directly affect the luminosity measurement. The largest such effect in Run I originated from time-dependent gain variations in the photomultipliers used to read out the HF. These gain changes can be at the few percent level, and translate into time dependent calibration changes of the luminosity values at the few percent level, necessitating recalibration.

The HF has undergone a complete replacement of its photodetectors during LS1 for radiation hard, Hamamatsu R7600U-200-M4 multi-anode tubes. During Run 1, a small fraction of anomalous signals associated to interactions of charged particles in the PMT windows was measured. These tubes will have a thinner optical window, reducing the anomalous signals by a factor of four. The multi-anode readout of the tubes also provides the ability to identify an anomalous signal by its timing information since these signatures are $\sim 5\,ns$ prior to the collision signal, typically in one of the readout channels only.

### *4.2. Backend electronics upgrade*

The HF backend electronics hosts the luminosity firmware algorithms and performs real-time histogramming of the data used in the luminosity measurement.

The HCAL back-end electronics has been upgraded in LS1 and based on commercial FPGAs and the MicroTCA standard. The main components of the backend electronics is the $\mu$HTR board and the AMC13 board. The data processing for the HF luminosity determination in the $\mu$HTR board will be split between the two FPGAs. The front FPGA will calculate the numbers of long-fiber cells over threshold and the total transverse energy observed during each bunch crossing. The front FGPA will transmit this information to the back FPGA via a unidirectional 3.6 gigabit copper link. The back FPGA then creates a set of histograms to collect the ingredients for the luminosity measurements as a function of LHC bunch number. The histogram integration period can be either internally counted or based on the Lumi Nibble timing synchronisation signals from the TCDS, decoded and distributed by the AMC13. At the end of each integration cycle, the histograms will be moved into a storage buffer, with redundant triple buffering capabilities, from which the BRIL DAQ source processor will read them via the IPBus.

The firmware and software for the $\mu$HTR has been designed to allow separate operation of the luminosity path and the trigger/DAQ path. The two data paths will be coupled only at the alignment of the data from the front-ends which will be reset only when required by clock changes or other effects. The luminosity system will have its own set of calibration lookup tables ( and the software stack is being designed to allow separate xDAQ applications and RCMS controllers to be responsible for the luminosity and trigger/DAQ activities of the uHTR. This separation will provide maximum flexibility for both systems, allowing the luminosity system to have the largest possible uptime while also granting operational simplicity for the trigger/DAQ operations.

## 5. Beam Halo Monitor

A Beam Halo Monitoring (BHM) system [17] has been designed to provide an online bunch-by-bunch measurement of MIB arriving CMS at a radius of 1.8 m from beam axis, separately for the two beams. At this location the detectors are sensitive to muon MIB arising from interactions in collimators in the long straight sections. The system is an array of fast, directional Cherenkov detectors that are distributed azimuthally outside the rotating shielding of CMS. The longitudinal location of 20.625 m from the IP as shown in Figure 11 (left), provides a maximum time separation of MIB from the collision products. The system will flag at real-time adverse beam conditions to CMS and LHC, complementing the measurement by the diamond-sensor based BCM1F system at lower radius and closer to the IP.

### *5.1. BHM Frontend Design and Qualification*

A BHM detector unit consists of the following components: Cherenkov radiator made from a synthetically fused quartz bar of 10 cm length and 5.1 cm diameter, black-painted on the front side; 1 mm optical coupling using RTV1345; a fast, UV sensitive photomultiplier

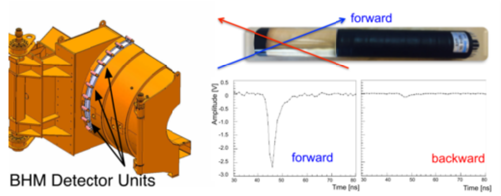


Figure 11: (left) BHM system installed around CMS rotating shielding (1/4 of installation). (right) Signal amplitude as a function of time show the different responses to forward and backward going particles.

R2059 from Hamamatsu; triple layer magnetic shielding consisting of 0.6 mm permalloy, 1 mm $\mu$-metal and 1 cm thick steel tube.

By exploiting the prompt and directional nature of Cherenkov radiation, the BHM system makes use of both timing and directionality to identify background. The digitized signal is characterized by 3.0 ns FWHM. The the signal amplitude depends on the direction of the incoming particle, as shown in Figure 11 (right). Each detector unit is orientated such that the incoming beam background from the tunnel will produce a large signal relative to collision products. The magnetic shielding serves both as a shield for the PMT from the 17 mT residual magnetic field and a shielding from low energy $e^-/e^+$produced by proton-proton collisions, arriving at the same direction with the MIB.

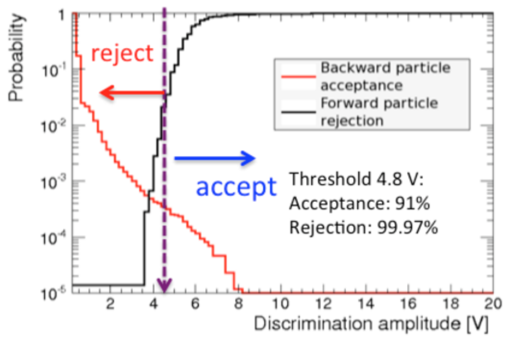


Figure 12: Normalized amplitude distributions from test beam data for forward and backward going particles.

The directional response of the BHM is used to suppress signals originating from collision products while selecting particles parallel and consistent with the direction of the incoming beam. This allows for an efficient MIB measurement. During test-beams it was validated that the suppression of the backward signal to 1 over 1000 is achievable; by setting a discrimination voltage, e.g. 4.8 V as shown in Figure 13, 91% of the forward signal is accepted, while the backward signal acceptance is suppressed to O(10-4).

The fronted units are radiation hard and are qualified for $> 3000\,\text{fb}^{-1}$ at this location.

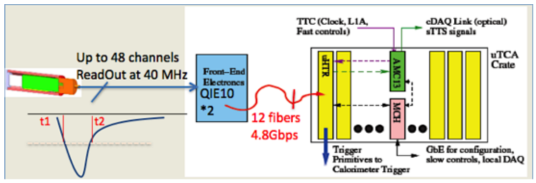


Figure 13: Overview schematic of the BHM Electronics.

### 5.2. *BHM Electronics*

The readout of the BHM detector will make use of many components developed for the CMS HCAL electronics upgrade [16], with dedicated firmware and readout adapted to the beam monitoring requirements [18]. The PMT signal will be digitized by a charge integrating ASIC (QIE10), providing both the signal rise time and the charge integrated over one bunch crossing. It ensures dead-timeless readout of signal amplitude and edge time information with 500 ps resolution.

The backend electronics will record histograms with few ns binning. The beam background rates will be published to CMS and the LHC. A calibration monitoring system has been designed to generate triggered pulses of light to monitor the efficiency of the system.

## 6. Data Acquisition and Synchronization

The BRIL DAQ system is presently under design and builds on the XDAQ[19], a C++ framework for distributed data acquisition, and the run-control framework of CMS. Similar to CMS central DAQ, the BRIL DAQ manages distributed and heterogeneous subsystems, using a homogeneous distributed software architecture, where reliability and redundancy are important to prevent unwanted down time. The event-driven architecture enables large numbers of loosely coupled software components and services to exchange information in near real-time.

To fully exploit the redundant online luminosity and beam background monitoring system, the BRIL subsystem histogramming frontends are synchronized using common timing signals distributed by the CMS TCDS system, defining the hit count integration interval boundaries. Long command counters are also distributed for additional for inter-system synchronization. Using such a technique uniforms the accounting of delivered luminosity and the down stream data handling of the BRIL DAQ.

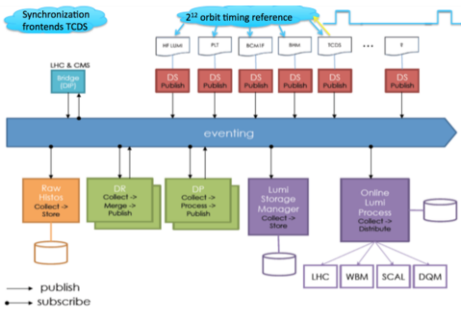


Figure 14: Schematic of the BRIL DAQ architecture based on XDAQ and a publisher / subscriber exchange of data via a common "eventing" bus.

BRIL DAQ components are logically categorized as a source, a processor or a central processor. A source is the hardware readout unit for each subsystem. A processor is responsible for local data aggregation and reduction, luminosity and beam background calculations. A processor component can collect, aggregate and further reduce data from various subsystems. Central processors serve for different purposes such as storage, luminosity selection or global online data quality monitoring. XDAQ b2in eventing in publisher/subscriber mode is used for data transport between these software components, as shown schematically in Figure 14.

There are multiple XDAQ processes running in the BRIL linux cluster. The global configuration and control of them will be achieved by a single generic function manager driving several configuration groups. The control of BRIL DAQ processes, which are stateless, and should run whenever there is beam in the LHC machine, independent of the state of the central CMS DAQ.

## 7. Conclusion

Upgraded beam instrumentation is being installed in LS1 to monitor the beam conditions for CMS for 2015. An online luminosity system consisting of three independent luminometers, the PLT, BCM1F and HF-luminosity readout, will ensure a robust measurement and accounting of the delivered luminosity and offers an advantage for the estimation of systematic errors. The upgraded BCM1F will enhance monitor beam background particles at low radius and the novel BHM system will complement with efficient measuring of the higher radius beam background.

The detector frontend readouts will be synchronized by common distributed timing signals and a data acquisition architecture is being developed to provide a common software framework for data processing, publishing and storage of synchronized data.

## References


[1] CMS Collaboration, *The CMS experiment at the CERN LHC*, JINST 3 (2008) S08004, doi:10.1088/1748-0221/3/08/S08004.

[2] Lyndon Evans and Philip Bryant, *LHC Machine*, 2008 JINST 3 S08001, doi:10.1088/1748-0221/3/08/S08001.

[3] Allkofer, Y et al, *Design and performance of the silicon sensors for the CMS barrel pixel detector*, Nucl. Instrum. Methods Phys. Res., A 584 (2008) 25-41

[4] M. Barbero et al., *Design and test of the CMS pixel readout chip*, Nucl. Instrum. Methods Phys. Res., A 517 (2004) 349

[5] R. Hall-Wilton et al *Results from a Beam Test of a Prototype PLT Diamond Pixel Telescope*, Nucl. Instrum. Methods Phys. Res., A 636 (2011) S130-S136

[6] M Pernicka et al *The CMS Pixel FED*, Topical Workshop on Electronics for Particle Physics, Prague, Czech Republic (2007), 487-491 doi 10.5170/CERN-2007-007.487

[7] R. Hall-Wilton et al *Fast beam conditions monitor (BCM1F) for CMS*, Topical Workshop on Electronics for Particle Physics, Greece, (2008) pp. 259-263

[8] A. Dabrowski et al., *The Performance of the Beam Conditions and Radiation Monitoring System of CMS*, proceedings IEEE Nuclear Science Symposium and Medical Imaging Conference, Valencia, Spain, 23 - 29 Oct 2011 DOI 10.1109/NSS-MIC.2011.6153979

[9] F. Vasey, *Development of radiation-hard optical links for the CMS tracker at CERN* IEEE Trans. Nucl. Sci. 45 (1998) 331-337

[10] N. Odell., *Measurements of Luminosity and Normalised Beam-Induced Background Using the CMS Fast Beam Condition Monitor*, in proceedings of ICHEP2012, PoS(ICHEP2012)526.

[11] J. Kaplon and W. Dabrowski, *Fast CMOS binary front end for silicon strip detectors at LHC experiments*, 2005 IEEE Transactions on Nuclear Science 52(6), pp.2713-2720.

[12] A. Fasso, A. Ferrari, J. Ranft, and P.R. Sala, *FLUKA: a multi-particle transport code*, CERN-2005-10 (2005), INFN /TC _ 05 /11, SLAC-R-773

[13] M. Penno, *A Real-time Histogramming Unit for Luminosity and Beam Background Measurements for each Bunch Crossing at the CMS Experiment*, TWEPP 2013 - Topical Workshop on Electronics for Particle Physics, Perugia, Italy

[14] A Zagozdzinska et al, *Architecture of the upgraded BCM1F Backend Electronics for Beam Conditions and Luminosity Measurement*, TWEPP 2014 - Topical Workshop on Electronics for Particle Physics, Proceedings, to be published in JINST

[15] E Hazen et al *The AMC13XG: a new generation clock/timing/DAQ module for CMS MicroTCA* (2013) JINST 8 C12036 doi:10.1088/1748-0221/8/12/C12036

[16] J. Mans et al, *CMS Technical Design Report for the Phase 1 Upgrade of the Hadron Calorimeter*, CERN-LHCC-2012-015, CMS-TDR-010

[17] S. Orfanelli et al, *Design of a Novel Cherenkov Detector System for Machine Induced Background Monitoring in the CMS Cavern*, Proceedings, 2nd International Beam Instrumentation Conference, Oxford UK, (2013) isbn = 978-3-95450-127-4

[18] N. Tosi et al, *Electronics and Calibration system for the CMS Beam Halo Monitor*, Proceedings, TIPP'14 conference, (2014)

[19] J. Gutleber, S. Murray, L. Orsini, *Towards a homogeneous architecture for high-energy physics data acquisition systems* Comput. Phys. Commun. 153 (2003), 155163 DOI: 10.1016/S0010-4655(03)00161-9